Photoacoustic spectroscopy applied to on-line measurement of carbon loadings in fluidized bed combustion flue gas

by

Jeffrey Raymond Dykstra

A Thesis Submitted to the
Graduate Faculty in Partial Fulfillment of the
Requirements for the Degree of
MASTER OF SCIENCE

Major: Mechanical Engineering

Iowa State University
Ames, Iowa
1990

TABLE OF CONTENTS

LIST OF TABLES

LIST OF FIGURES

NOMENCLATURE

A_a	=	Mass specific absorption coefficient
A_e	=	Mass specific extinction coefficient
b_a	=	Absorption coefficient
b_e	=	Extinction coefficient
C_a	=	Absorption cross section
C_p	=	Particle heat capacity per unit volume
C_s	=	Scattering cross section
D	=	Diameter
$\bar{D}$	=	Mean diameter
$f(D)$	=	Diameter frequency distribution
k_a	=	Thermal conductivity of air
L	=	Optical path length
$m(D)$	=	Mass distribution
M_c	=	Carbon mass loading
M_t	=	Total mass loading
N	=	Total number of particles per unit volume
R	=	Responsivity of the photoacoustic spectroscopy cell
$\bar{r}$	=	Mean radius

R_a	=	Mass specific absorption cross section
R_e	=	Mass specific extinction cross section
S	=	Photoacoustic spectroscopy signal
V	=	Volume of photoacoustic spectroscopy cell
W	=	Optical power

Greek Symbols

α	=	Ratio of specific heats
λ	=	Wavelength
ρ	=	Density
σ_m	=	Microphone sensitivity
τ	=	Thermal time constant
ω	=	Angular modulation frequency

ACKNOWLEDGEMENTS

Special thanks go to Professor Robert Brown for his insight and advice throughout my research. I would also like to thank Dr. Jon Van Gerpen and Dr. Thomas Wheelock for serving on my graduate committee. I would also like to thank Nathan Rozenboom for the work done machining the PAS cell.

I would like to thank my parents, Martin and Ruthanne Dykstra, for their support and encouragement. I would also like to thank my sisters—Jaye, Joni, and Jennifer; their words of encouragement were greatly appreciated. The encouragement of my friends at Iowa State and Unity Christian Reformed Church provided strength when problems were encountered. Special thanks to Lynne Koerselman for her support and understanding, especially in the final months of this project.

This work was supported by the Iowa State University Engineering Research Institute and the Iowa State Mining and Mineral Resources Institute.

1. INTRODUCTION

The manual loss-on-ignition (LOI) test used to determine the percent unburned carbon in fly ash is a tedious and sometimes inaccurate procedure [1]. Fly ash sampled from the exhaust of a combustor is dried and weighed before being subjected to an ashing furnace for several hours at 725 °C. The sample is then reweighed; the change in weight is assumed to be due to the carbon present in the sample. The accuracy of this technique is limited by the assumption that only carbon in fly ash changes weight upon heating. However, fly ash may contain other constituents that change weight upon heating. For example, calcium carbonate, commonly injected into combustors as a sulfur sorbent, can appear in fly ash. The conversion to calcium oxide upon heating is accompanied by a 44% reduction in the original weight of the sample.

An innovative and promising concept for on-line determination of carbon loading in coal combustion flue gas is photoacoustic spectroscopy (PAS). The photoacoustic effect is manifested as an acoustical wave that is produced when amplitude modulated radiation is absorbed by the gas or by particles suspended in a gas. The energy absorbed by the sample is transferred as heat to the surrounding gas, resulting in a minute temperature rise. Subsequent expansion of the heated gas causes a periodic pressure fluctuation at the modulation frequency, which propagates through the gas as an acoustical signal.

PAS work done with soot particles [2, 3] suggests that PAS would also be suited to the challenge of on-line determination of carbon loading because the PAS signal is based solely on the absorption of radiation and not on the energy lost from the incident beam due to absorption and scattering. Although elutriated carbon from coal combustion differs from diesel soot in both particles size and morphology, the technique has features that should allow the transition from diesel exhaust to fly ash. Dona and Brown have shown, using synthetic fly ash, that the PAS signal is linearly dependent on the carbon concentration in the sample [4, 5].

The radiation source for this project is a He–Ne laser ($\lambda = 632.8\ \eta$m). At this wavelength, combustion gases and mineral matter in the fly ash should not absorb appreciably compared with the strong absorption of radiation by the carbon particles [5, 6]. With these assumptions, the PAS signal produced is generated solely on the carbon loading and does not depend on the combustion gases or other particles present in the flue gas.

The goal of this research was to determine if the noise limit for the PAS system can be reduced (Dona and Brown—signal-to-noise ratio of 2 [4, 5]), and if the PAS signal is linearly proportional to the unburnted carbon concentration in the fly ash generated from a laboratory-scale fluidized bed. The characteristics of unburned carbon particles will be studied to lend insight into how the PAS system can be optimized. A PAS apparatus was designed and installed on a laboratory-scale fluidized bed combustor to determine the advantages and disadvantages of the PAS technique.

2. DEVELOPMENT OF PHOTOACOUSTIC SPECTROSCOPY

The photoacoustic effect in both gaseous and non-gaseous matter was discovered by Alexander Graham Bell in 1880. Photoacoustic studies, however, remained dormant until the advent of the laser in the early seventies, which provided a powerful excitation source. Photoacoustic applications were first limited to the study of gases and aerosols but have recently been expanded to the study of solids [7, 8].

2.1 Particle Interactions with Radiation

The interaction between particles and radiation depends on the complex index of refraction of the particle, the diameter of the particle, and wavelength of the incident radiation. Both scattering and absorption can occur; the sum of these two quantities is called extinction. A measure of the amount of scattering or absorption is given by the scattering cross section, C_s, or the absorption cross section, C_a, which are based on the above parameters. In the study of particles, it is convenient to express particulate properties on a mass basis. The absorption cross section on a mass basis for a single-sized particle system is [9]

$$R_a = \frac{C_a}{\rho(4/3)\pi(D/2)^3} \tag{2.1}$$

where R_a is defined as the absorption cross section per unit mass of a particle of diameter D, and ρ is the particle density.

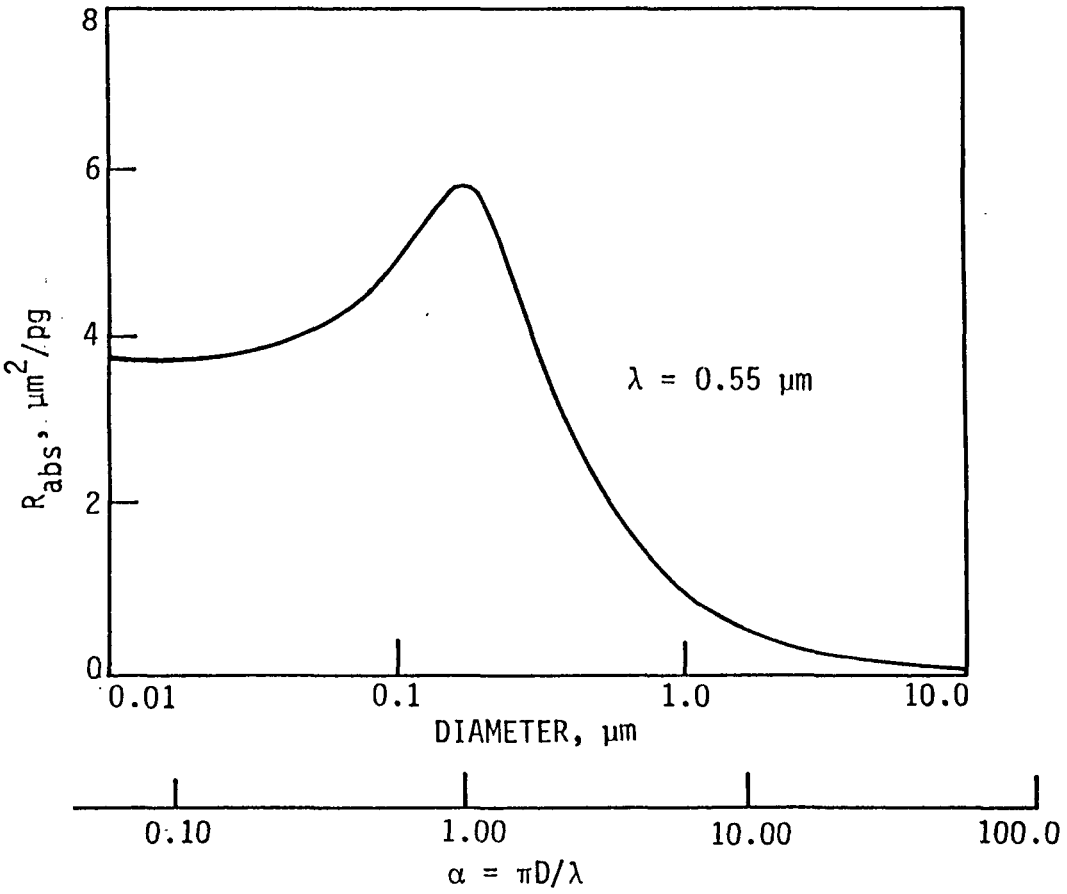

Figure 2.1: Mass specific absorption cross section for carbon particles at 0.55 μm

Faxvog and Roessler [9, 10] calculated R_a as a function of particle size. Their results are presented in Figure 2.1 as R_a versus particle size. For Rayleigh particles ($D \ll \lambda$) the mass specific absorption cross section, R_a, is independent of particle size. In the limit of large particles ($D \gg \lambda$), R_a is inversely proportional to the particle diameter and can be estimated by [11]

$$R_a \approx \frac{3}{2}\left(\frac{1}{\rho D}\right) \tag{2.2}$$

Since fly ash is not monodisperse in size, R_a must be adjusted to account for

the effects of a size distribution. The absorption coefficient, b_a, takes into account a particle size distribution [9]

$$b_a = \int_0^\infty R_a(D)m(D)dD \tag{2.3}$$

where

$$m(D) = \rho(4/3)\pi(D/2)^3 N f(D) \tag{2.4}$$

such that

$$\int_0^\infty m(D)d(D) = M_c \tag{2.5}$$

where $f(D)$ is the diameter frequency distribution, N is the total number of absorbing particles, and M_c is the mass concentration of absorbing particles. Combining Eq. (2.3) and Eq. (2.5) produces an expression for the mass specific absorption coefficient, A_a

$$A_a = \frac{b_a}{M_c} = \frac{\int_0^\infty R_a(D)m(D)d(D)}{\int_0^\infty m(D)d(D)} \tag{2.6}$$

where A_a was chosen to be based on the mass concentration of absorbing particles and not on the total mass concentration.

The only restriction on the previous discussion is that multiple scattering does not occur. This is, all particles in the particle cloud interact independently with the incident radiation. This restriction is satisfied if the condition

$$M_t < \frac{1}{A_e L} \tag{2.7}$$

is met [11], where M_t is the total mass concentration, A_e is the mass specific extinction coefficient, and L is the length of the PAS cell. For large mean particle diameters [9]

$$A_e \approx R_e \tag{2.8}$$

where [11]

$$R_e \approx 3\left(\frac{1}{\rho D}\right) \tag{2.9}$$

Using standard values for fluidized bed combustion fly ash—$\bar{D} = 20$ μm (a conservative estimate) and $\rho = 2000$ kg/m^3,—Eq. (2.7), Eq. (2.8), and Eq. (2.9) with $L = 0.1$ m, suggest that the mass loading must be less than 130 g/m^3. A mass loading of 130 g/m^3 is far above the mass loading expected from a bubbling fluidized bed combustor [12]. Therefore, dilution of the combustion exhaust is not necessary to meet this criterion.

2.2 The Photoacoustic Signal

The photoacoustic technique is based on periodic absorption of radiation from a modulated source. The energy absorbed by the sample is converted to heat, which results in a minute temperature rise in the surrounding gas. Subsequent expansion of the heated gas causes periodic pressure fluctuations at the light modulation frequency, which propagates through the gas as an acoustical signal. This signal can be detected by an appropriately sensitive microphone and a lock-in amplifier [7, 8].

To enhance the photoacoustic effect for absorption measurement, the sample is contained in a gas-filled chamber, the photoacoustic cell. Roessler and Faxvog [13] derived an equation for the photoacoustic signal, S, for non-resonant operation with the assumption that the pressure rise is uniform throughout the cell:

$$S = R(b_a/b_e)[1 - e^{-b_e L}]W/L \tag{2.10}$$

where R is the cell responsivity (mV-m/W), b_a is the absorption coefficient (m^{-1}), b_e is the extinction coefficient (m^{-1}), L is the optical path length of the sample (m), and

W is the optical power incident on the sample (W). For the case of weak attenuation, $b_e L \ll 1$, Eq. (2.10) simplifies to

$$S \approx R b_a W \tag{2.11}$$

and on a mass basis

$$S \approx R A_a M_c W \tag{2.12}$$

where M_c is the mass concentration of absorbing particles in the sample and A_a is the mass specific absorption coefficient based on the absorbing particles in the sample.

Both Eq. (2.11) and Eq. (2.12) show that the signal is proportional to the cell responsivity and laser power. Responsivity, a measure of the instrument gain, is a function of cell geometry and material, modulation frequency, and microphone sensitivity. The theoretical cell responsivity, R, for non-resonant operation is [13]

$$R = \frac{4(\alpha - 1)\sigma_m L}{\pi \omega V \sqrt{2}} \tag{2.13}$$

where α is the ratio of specific heats (C_p/C_v), σ_m is the microphone sensitivity (mV/Pa), L is the optical path length of the photoacoustic cell (m), V is the total volume of the cell (m^3), and ω is the angular modulation frequency (s^{-1}).

Eq. (2.13) shows that low frequencies give the highest responsivity; however, the magnitude of the background noise is less at higher frequencies [3, 14]. The theoretical upper limit for the modulation frequency is given by the thermal time constant τ [15]

$$\tau = \frac{r^2 C_p}{3 k_a} \tag{2.14}$$

where r is the particle radius, C_p is the heat capacity per unit volume of the particle, and k_a is the thermal conductivity of the air or surrounding medium. This limit assumes that the entire particle is heated uniformly, which is satisfied for soot particles

($\bar{r} \sim 0.1$ μm). However, research done with carbon particles ($\bar{r} \sim 50$ μm) show that frequencies higher than this limit can be used effectively [5]. When using frequencies higher than this limit, the entire particle is no longer heated, but only the outside surface.

The thermal time constant requires that the modulation frequency to be less than 50 Hz for the size of particles involved in this study. At a frequency of 50 Hz, the noise interference would be so great that the PAS signal could not be detected. Therefore, it is advantageous to exceed this limit to increase the signal-to-noise ratio to a workable level.

In practice, cell responsivity can be determined by using Eq. 2.11 and a gas with well defined absorption characteristics; nitrogen dioxide is a convenient gas for this purpose [2, 13, 14].

2.3 Diesel Exhaust Measurements

Previous experimental work in measuring soot of diesel exhaust emissions with PAS serves as a starting point in designing a PAS system for measuring unburned carbon. A PAS system for the measurement of soot in diesel vehicle exhaust consists of a constant flow dilution tube, horizontal PAS cell, microphone, signal processing equipment, and a modulated radiation source [16]. The combustion products enter a constant flow dilution tube where the dilution ratio is 3:1 to 10:1, depending on engine operating conditions. This dilution assures isokinetic sampling without having to change the flow rate through the PAS cell. The microphone picks up the acoustic signal, and the signal is processed by a lock-in amplifier to extract the PAS signal.

The PAS method is suited for the detection of soot in diesel exhaust because

carbon in soot is comprised of about 1% trace metals from fuel and lubrication oil additives and about 2% sulfates, neither of which contribute significantly to the photoacoustic signal. The remaining material, greater than 95% by mass, is carbonaceous in nature, a strong absorber of radiation [2].

If the mass specific absorption coefficient, A_a, remains constant, the signal will have a direct correlation to the mass concentration of the material in the sample. Roessler and Faxvog [17, 18] found that the mass specific absorption coefficient for diesel particles varied with operating conditions up to a factor of two. Although the mass specific absorption coefficient for diesel particles varied with operating conditions, Japar, Szkarlat, and Pierson [19] found the mass specific absorption coefficient of the elemental carbon in the exhaust did not vary significantly with vehicle operating conditions. Therefore, if A_a is based on the mass concentration of absorbing particles, M_c, and not on the total mass concentration, M_t, the PAS signal can give quantitative information about the mass loading of elemental carbon in vehicle exhaust.

Two different radiation sources have been evaluated for measuring soot: CO_2 and argon–ion lasers. CO_2 lasers ($\lambda = 10.6$ μm) have been used to satisfy Rayleigh scattering criteria ($D \ll \lambda$); but at this wavelength, gaseous combustion products also absorb the infrared radiation and produces a significant photoacoustic signal. A two cell photoacoustic device was needed to subtract out the combustion gas contribution to the signal [2, 6, 20]. With the dual-cell setup, care must be taken to insure that gaseous components going through each cell are equivalent; one flow with soot particulates and the other flow with soot particulates filtered out [2, 6, 20].

PAS research with argon–ion lasers ($\lambda = 0.515$ μm) shows that light absorption

by soot particulates can be approximated as Rayleigh scattering [2, 3]. The advantages of working at this wavelength are two fold. First, the mass specific optical absorption coefficient A_a is about an order of magnitude greater at this wavelength, resulting in a direct gain in the PAS sensitivity. Second, the duel-cell method is no longer needed because combustion gases do not absorb appreciably at visible wavelengths; hence they do not contribute to the photoacoustic signal [6].

Roessler has worked with resonant [3] and non-resonant [21] PAS systems. Although the sensitivity can be increased by using a resonant system, the system must be continually tuned to keep the PAS cell in the resonance mode, due to small variations in temperature and flow rate through the PAS cell. Although temperature affects the frequency at which the cell operates in the resonant mode, there is no affect on the non-resonant PAS signal for temperatures above 28 °C [22]. The non-resonant PAS system provides better calibration stability and allows for changes in the flow rate through the PAS cell without affecting the calibration [20]. Therefore, Roessler [21] chose to work with the non-resonant PAS system.

2.4 Carbon Detection in Synthetic Fly Ash

The detection of unburned carbon in fly ash differs from the detection of soot in diesel engines because the size of the fly ash particles is at least an order of magnitude larger than soot. This affects the absorption of the incident radiation (Section 2.2). The larger size also requires more care be taken to keep the particles entrained in the air flow.

Brown and Dona [4, 5] have used photoacoustics to measure carbon in airborne synthetic fly ash. Their experimental setup is similar to that used for soot measure-

ments [16] except that (1) vertical orientation of the photoacoustic cell was used, (2) no constant flow dilution tube was used with the particulate supply system, and (3) the radiation source was a He–Ne laser ($\sim$ 35 mW compared with 500–1000 mW for argon–ion or CO_2 lasers). If a horizontal configuration was used, the air velocity would need to be very high to keep the particles entrained in the air stream. Osada et al. [20] show that photoacoustic response is independent of gas flow rate only for relatively low flow velocities. They suggest that flow velocities should be less than 0.40 m/s through the cell. The vertical orientation of the cell prevents particles from settling out of the air flow while maintaining a relatively low flow velocity through the cell. Brown and Dona used a fluidized bed to entrain the synthetic fly ash in the air before passing it through the PAS cell. Synthetic fly ash is a combination of Illinois No. 5 coal, screened to 270- by 325-mesh, and pulverized coal fly ash that has been previously heated in an oxidizing environment to remove all carbon. Synthetic fly ash differs from actual fly ash in that the carbon did not passed through a combustion zone and is monodisperse in size. With a total mass loading of 2 g/m^3, Brown and Dona [4, 5] were able to measure carbon-in-fly ash between 30% to 100%. Acoustical noise overwhelmed the PAS signal at carbon concentrations below 0.6 g/m^3, which is around the upper limit expected from industrial-scale fluidized bed combustors.

3. FLUIDIZED BED FLY ASH

Fly ash consists of the material that is elutriated from the combustor. Fly ash is comprised of ash and small char particles. The shape, size distribution, and morphology of the fly ash are important parameters for the PAS technique because these properties affect the mass specific absorption coefficient for the fly ash particles.

The chemical characterization of the ash in fly ash is substantially due to properties of the coal being used. Mineral matter in the coal is comprised of clays, shales, pyrite, quartz, calcite, and lesser amounts of other materials [23]. Predominately, mineral matter takes two forms in the coal: finely disseminated, generally submicroscopic particles and relatively coarse mineral inclusions. The first form includes the inorganic constituents of the original coal-forming plants, and the second form is comprised of various minerals washed in with the coal-forming material [24]. Only the first form is important to the PAS signal. The latter form of the mineral matter either stays in the bed or is elutriated as ash particles, which have a very low mass specific absorption coefficient and produce a negligible signal. In the first form, where the mineral matter is finely disseminated, it may stay attached to a carbon particle and shade the carbon from incident radiation passing through the PAS cell. Donsi, Massimilla, and Miccio [25], using an optical microscope, describe some fly ash particles as having heterogeneous structures that are comprised of ash and carbon.

When a particle is comprised of both ash (small absorption coefficient) and carbon (large absorption coefficient) the effect on A_a (mass specific absorption coefficient) is unknown.

The discussion on particle interaction with radiation in Chapter 2 assumes spherical particles. Unlike pulverized coal combustors, fluidized bed combustors produce non-spherical fly ash particles. In addition, with pulverized coal combustors, the ash fusion temperature is reached and the ash forms droplets that later solidify to a spherical shape. On the other hand, with fluidized bed combustors, temperatures are usually below ash fusion temperatures, resulting in irregularly shaped fly ash particles [26, 27]. This does not invalidate the use of the PAS technique, but makes the values of the PAS signal hard to predict.

The particles size distribution influences the mass specific absorption coefficient, A_a. With fluidized bed combustors, the mean size of the fly ash is almost solely dependent on the operating conditions (temperature, excess air, superficial gas velocity, and fly ash recycle) and only weakly dependent on the coal type [28, 29]. Two frequency distributions have been postulated—one distribution less than 100 μm and another distribution greater than 100 μm—where the largest size present in the fly ash is dependent on the gas velocity above the minimum for fluidization and on the recycle of the fly ash [28, 29, 30, 31]. With high recycle of the fly ash, the mean particle diameter of the fly ash decreases significantly [26, 29]. Merrick and Highley [29] report that the size distribution of fines produced is approximately constant for a particular bed material and is independent of the bed size distribution or operating conditions of the fluidized bed combustor. In the second distribution, particles that are greater than 180 μm contain mostly unburnt carbon particles [32].

4. EXPERIMENTAL APPARATUS

The experimental apparatus consists of two main systems: the fluidized bed combustion facility and the photoacoustic absorption spectroscopy (PAS) apparatus.

4.1 Fluidized Bed Combustion Facility

The fluidized bed combustion facility provided all the fly ash used in this study. The facility consists of the following five components: fluidized bed combustor, exhaust system, gas analysis, fuel supple system, and data acquisition.

4.1.1 The Fluidized Bed Combustor

A schematic of the 8-inch diameter fluidized bed combustor is shown in Figure 4.1. The distributor plate consists of 250 3/32-inch diameter holes evenly distributed in 1/2-inch stainless steel. Spot welded to the distributor plate is a 100-mesh stainless steel screen. This screen acts as a flame arrestor and prevents bed material from falling into the plenum. During the preheat stage, the plenum allows liquefied petroleum gas (LPG) and the primary air to mix vigorously before being ignited by an electrode sparker.

The inner wall of the combustion bed is made of stainless steel lined with a 1-inch thick layer of castable refractory. Heat is removed from the bed by a water jacket

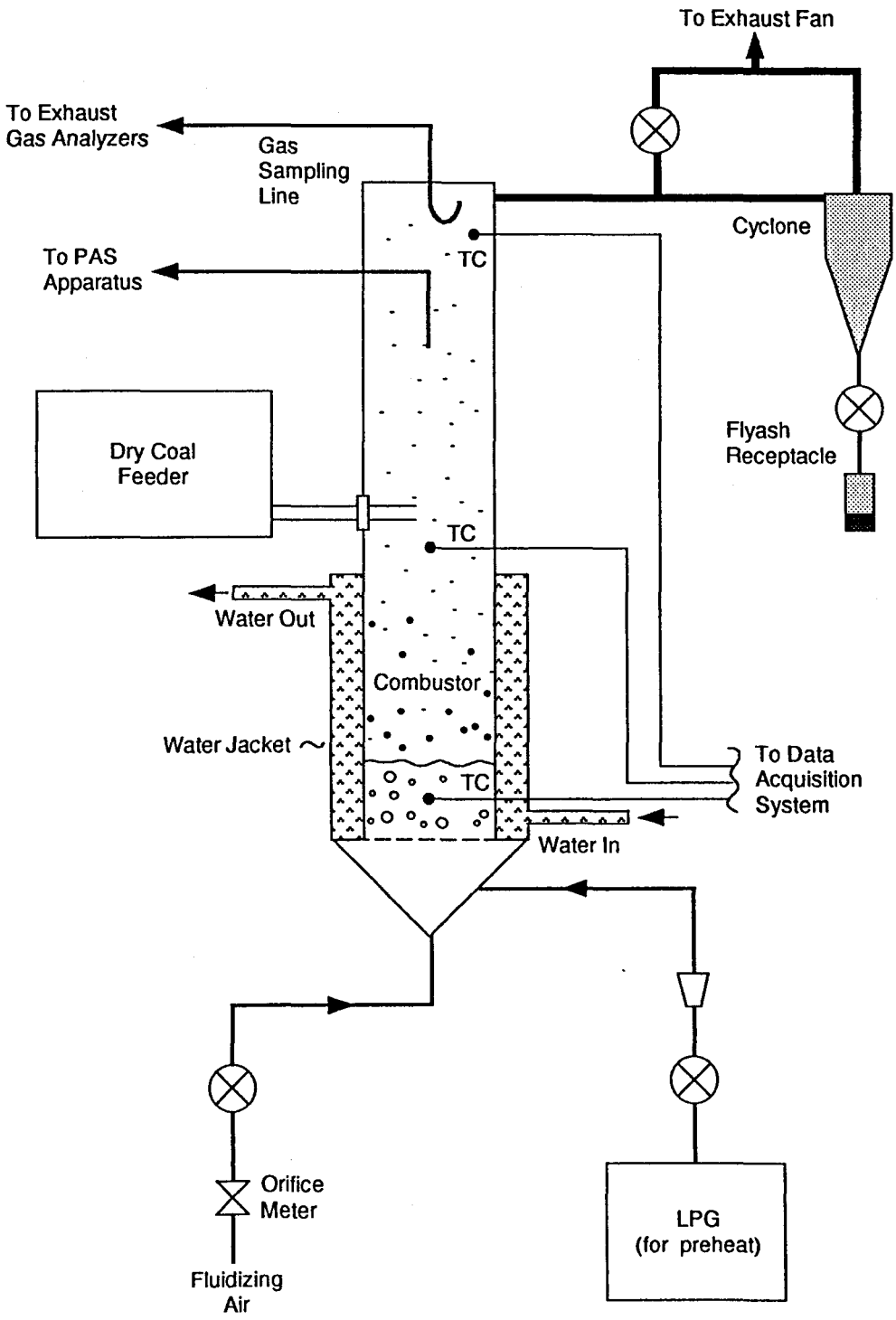

Figure 4.1: The fluidized bed combustor

surrounding the bed. An uninsulated, mild-steel freeboard extends 4-feet above the combustion bed, which reduces elutriation losses.

4.1.2 The Exhaust System

Flue gas exits from the top of the combustor through a high efficiency cyclone that captures over 97% (on a mass basis) of particles produced by the combustor [33]. Two probes are used for particle and gas sampling. The first probe is a 1/2-inch mild steel pipe that descends 12-inches down the center of the freeboard and provides isokinetic sampling of the fly ash. The second probe consists of a 1/4-inch stainless steel probe directed away from the combustion bed to reduce the amount of fly ash entering the exhaust gas sampling tube. This port leads to the gas analyzers, which determine the exhaust gas composition.

4.1.3 Gas Analysis

Exhaust gas sampled from the combustor is cooled and dried before passing to the gas analyers. The temperature of the sample line is maintained at 350 °F to prevent condensation of corrosive acids. Particulates are removed by passing the exhaust gas through a Balston type 30/12 particulate filter. The exhaust then passes through an acid mist filter and a Perma-Pure heatless drier. (The water vapor is removed so that the gases may be evaluated on a dry basis.) The exhaust then passes through a coalescing particulate filter and a vacuum pump before reaching the gas analyzers.

The gas analyzers provide continuous measurement of five exhaust gases: CO, CO_2, O_2, SO_2, and NO_x. Two Beckmann Model 820 non-dispersive infrared spec-

trometers are used to measure CO and CO_2 concentrations. A Beckmann Model 755 oxygen analyzer measures O_2 concentrations. Two Horiba model VIA-500 and VIA-300 non-dispersive infrared spectrometers are use to measure SO_2 and NO_x concentrations, respectively.

4.1.4 Fuel Supply System

Experiments were performed using an Indiana coal with 5% ash. The coal was crushed and screened to a top size of 3/8-inch and a bottom size of 8-mesh. Coal larger than 3/8-inch binds the feeder, whereas a bottom size of 8-mesh reduces the amount of fines in the fuel supply that will elutriate from the bed. To reduce the moisture content of the coal, the coal was allowed to dry in the open air for 24 hours before combustion. The crushed coal was metered into the combustor by an AccuRate dry chemical feeder (model 602), equipped with a 3/4-inch diameter, variable speed helix and a 5 gallon vinyl hopper. The feeder provides feed rates of coal from 1 to 50 pounds per hour. The hopper was sealed during combustor operation to prevent hot combustion gases from passing through the fuel supply and into the laboratory. The sealed feeder results in a maximum supply of 50 pounds of coal.

4.1.5 Bed Material

Two sets of tests were performed. The first set was performed with a 30- x 40-mesh sand bed to which 5% of 20- x 40-mesh limestone had been added to prevent tar formation in the combustor. Porous materials, such as fresh or spent limestone, are known to catalyze the destruction of tars released from coal during devolatilization [34]. However, as described in the results, this small quantity of limestone quickly

attrited and elutriated before the first set of tests were completed. The second set of tests was performed in a bed that was initially charged with 31% sand and 69% limestone. Limestone is not an ideal catalyst of tar for these tests because, as explained previously, it affects loss-on-ignition, which is used to check the unburned carbon content of fly ash in the experiments. Accordingly, all limestone in the bed material was calcined or sulfated by heating the bed with LPG and high-sulfur coal for two hours before performing PAS tests. The LOI for bed material after this bed conditioning was only 0.7%, compared with 27% for raw limestone, suggesting that very little uncalcined stone remained in the bed.

4.1.6 Data Acquisition

Temperature, air flow rates, and gas concentrations were monitored using a microcomputer, and are stored on hard disk every 5 seconds. Temperatures were measured by chromel/alumel (type k) thermocouple probes at locations at the bottom and top of the freeboard and within the bed. The probes were connected to a Metrabyte model EXP-16 sub-multiplexer board to amplify the voltage signal and provide cold junction compensation. The analog output from the EXP-16 was converted to a digital signal using a DAS-8 analog/digital converter interface board, which calculates and displays the temperature corresponding to each region in the bed.

Airflow through the bed was calculated from pressure drops across orifice flow meters. A linear variable displacement transformer pressure transducer was used to measure the pressure drop across the orifice meter. The analog output of the transducer was converted by a DAS-8 A/D converter. The digital signal was used by

the microcomputer to convert the pressure drop to a corresponding flow rate using calibration test data.

The gas analyzers have an analog output; a DAS-8 A/D converter makes the signal acceptable to the microcomputer. The channels containing the information for the gas concentrations, temperature, and airflow are all read by the computer at the same time, every 0.4 seconds.

4.2 PAS Apparatus

Two PAS cells, illustrated in Fig 4.2, were analyzed in this study. Both were designed to detect the relatively large particles of unburned carbon generated during combustion. Although PAS cells are generally constructed for horizontal flow, these cells use a vertical orientation to prevent particles from settling out of the flow stream. In order to keep particles from settling on the bottom window of the PAS cell, a small amount of purge air was introduced at the bottom of the cell.

The first cell, constructed from a solid block of aluminum, has a central chamber 13 mm in diameter. A flat window at the top of the cell admits the laser beam, which traverses the cell and exits through a Brewster window at the bottom. Particle-laden gas enters perpendicular to the laser path. In contrast, the second cell, constructed of a solid block of brass, has a central chamber only 4 mm in diameter. Brewster windows at both the top and bottom provide maximum transmission of the laser beam through the cell by minimizing beam reflections, scattering, and absorption at the windows. This reduces noise that would otherwise be produced due to absorption at the windows and the interaction of scattered radiation with the cell walls. The flow passage for the flue gas entering the cell was angled upward to reduce eddy currents

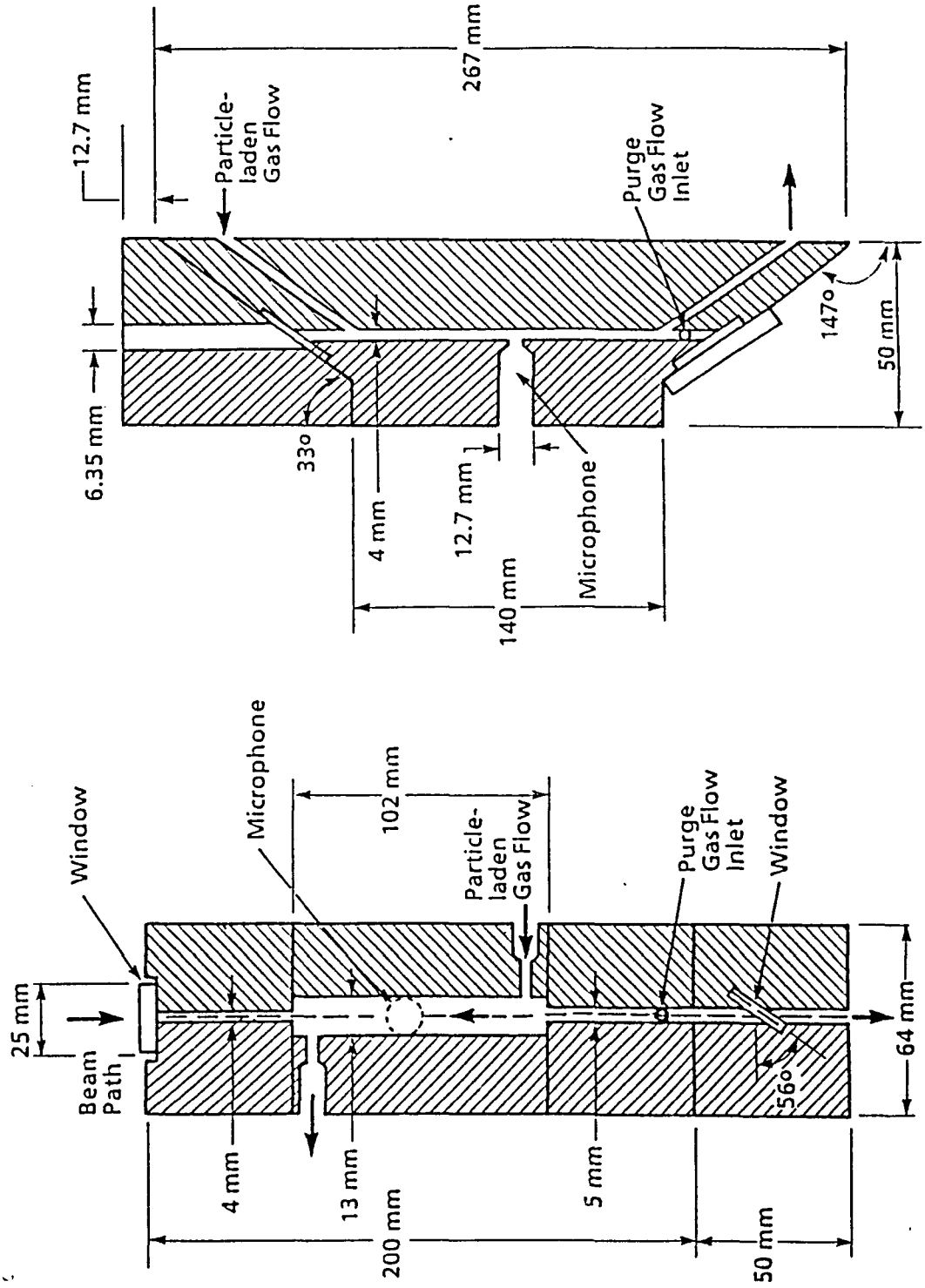

Figure 4.2: The aluminum and brass PAS cells

which generate acoustical noise in the cell. The smaller cell diameter is expected to increase cell responsivity of the cell (Eq. (2.13)), thereby providing a larger PAS signal (Eq. (2.12)).

A microphone, recessed into the cell wall in the middle of the central chamber is part of a General Radio model 1933 precision sound-level meter and analyzer. The half-inch electret condenser microphone has a sensitivity of -43 dB referenced to 1 V/Pa. The microphone is sealed into the PAS cell by using vacuum grease; a tightly woven cloth covers the microphone to protect it from fly ash particles.

The PAS cell is housed in an acoustical box inside a second acoustical box to isolate the cell from background room noise. The outer box is constructed of 3/4-inch plywood and is lined with 1.5 inches of foam. The inner box is constructed of 1/2-inch plywood, lined with 2 inches of fiberglass. All openings in the boxes for sample lines are packed with foam.

A flow schematic for the PAS apparatus is shown in Figure 4.3. Flue gas is sampled isokinetically from the freeboard of the combustor. To prevent condensation in the sample line, the sample line leading to the combustor is heat traced to a temperature of 150 °F, and the cell is maintained at 120 °F. Temperatures higher than 120 °F are not recommended for the microphone. Dilution gas can be added to the sample so that different mass loadings can be obtained for steady-state operating conditions. The flue gas sample passes though a muffler [35] consisting of a 3-inch pipe lined with 1-inch of fiberglass held in place by 40-mesh stainless steel. The muffler helps to isolate the PAS cell from noise generated during combustion. The sample for PAS analysis is extracted isokinetically along the axis of the muffler.

The sample is routed to the PAS cell where it passes through the beam of a

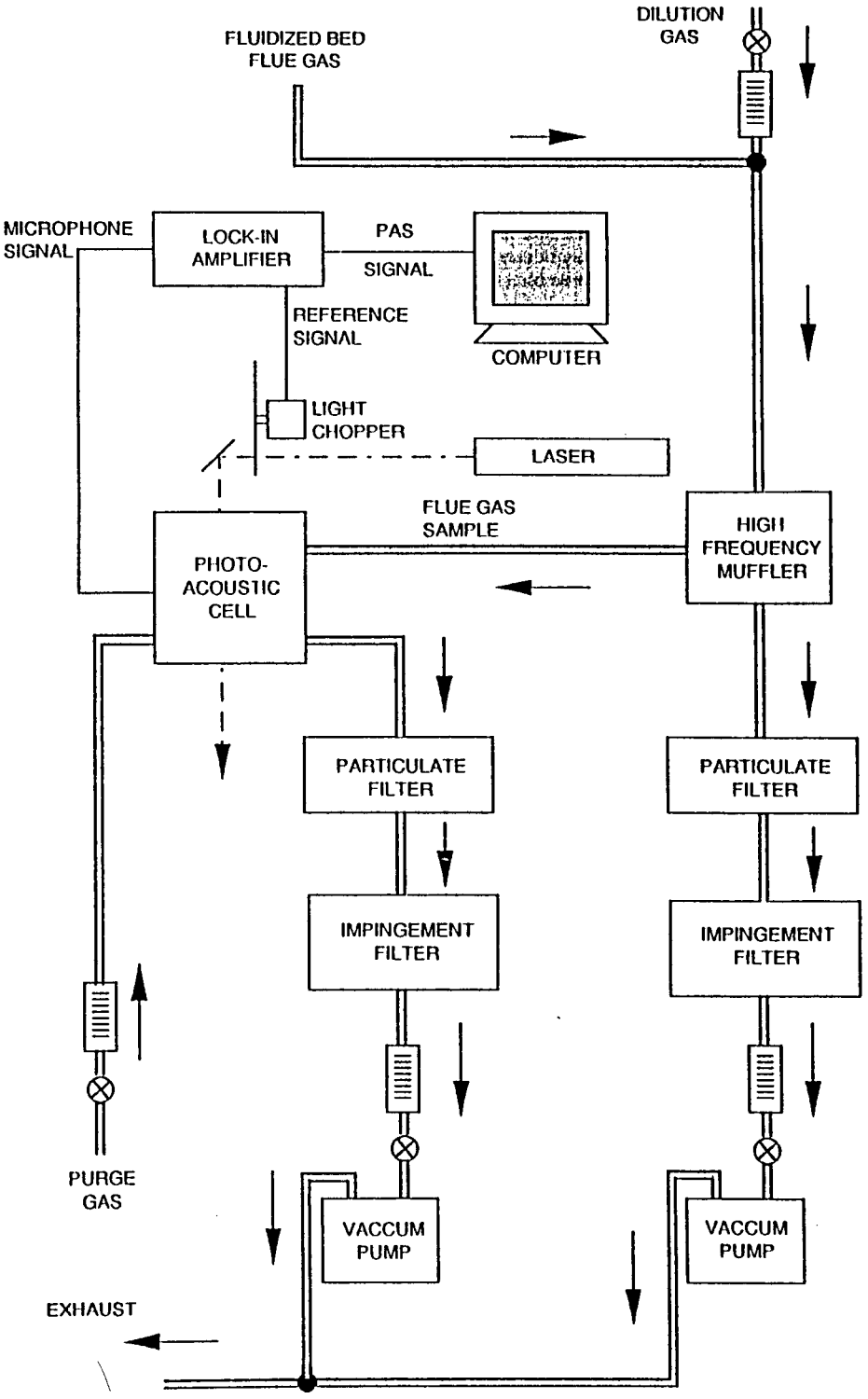

Figure 4.3: Flow schematic for the PAS apparatus

He–Ne laser that is modulated by an optical chopper. The optical chopper also provides a reference signal to the lock-in amplifier. Power into the cell was approximately 26 mW based on power meter measurements at the laser aperture and estimates of reflection and absorption losses at mirrors and windows. A lock-in amplifier extracts the PAS signal from the microphone signal, which is stored on the computer as an 8-bit character and as a function of time for subsequent analysis.

The solids in the flue gas sample are removed by a particulate filter before the gas sample reaches the pump. The sample collected on the filter is not large enough to determine LOI. As a result, LOI is performed on the cyclone catch, which is assumed to have the same distribution of carbon as passes through the PAS cell. This assumption is valid if isokinetic sampling conditions prevail. After the particle filters, the sample lines are no longer heat traced; an impingement filter is used to condense out the water vapor to prevent condensation from occurring in the flow meters.

5. PROCEDURE

5.1 General

Before every test, all samples lines were blown out with air, and the PAS cell was cleaned. Cleaning of the cell was usually unnecessary but occasionally there would be one or two large particles on the bottom window of the cell. The laser and the lock-in amplifier require at least one hour of warm-up time before the experiment may be performed. The laser was aligned through the PAS cell with the aid of a photovoltaic cell placed below the bottom window of the PAS cell. The voltage output from the photovoltaic cell corresponds to the intensity of radiation on the photovoltaic cell, thereby allowing for easy alignment of the laser.

5.2 PAS Cell Calibration

Calibration of the PAS cell was performed using 473 ppm NO_2 diluted in N_2 ($b_a = 0.028$ m^{-1} [36]). The calibration gas was transferred from a pressurized tank to an in-line plastic bag, where the gas was allowed to expand to atmospheric pressure. The gas was then pumped through the PAS cell at different flow rates, and the corresponding PAS signal was measured. The cell responsivity, R, can be calculated using Eq. (2.11). The calibration gas was than purged from the system, and air was pumped through the system, and the corresponding signal was measured. The

signal-to-noise ratio was taken to be the ratio of the PAS signal of calibration gas to the signal generated in the presence of air.

5.3 Carbon Concentration Measurements

Before the start-up of the combustor, the gas analyzers where checked to see if calibration was needed. The fluidized bed was then preheated with LPG. Coal was gradually added and the LPG gradually lowered until steady operation was achieved with coal at a desired fluidizing velocity and percentage of O_2 in the flue gas. Samples were extracted isokinetically from the combustor, diluted with air as desired, and passed through the PAS apparatus. Combustion stoichiometry was held constant at 4% oxygen in the flue gas for the first set of tests and 5% for the second set. Superficial velocity and bed temperature, both important parameters affecting particle size and morphology, varied during these tests.

6. RESULTS AND DISCUSSION

6.1 Acoustical Noise Reduction

Prior to the successful operation of the PAS cell, acoustical noise needed to be reduced. The effects of acoustical noise are two fold. First, the magnitude of these pressure waves can cause overloading of the microphone and the lock-in amplifier. Second, the PAS sensitivity is limited by noise interferences at the same frequency as the modulation frequency. These interferences include noise generated by: the absorption of radiation by cell windows and the cell wall, room noise, flow noise, and pressure waves generated by the pump and the combustor that propagate through the sample line into the PAS cell. A bandpass filter can significantly reduce noise, but additional methods are needed to increase the signal-to-noise ratio to a reasonable value.

Brewster windows can reduce the noise produced by the absorption of radiation by cell windows by minimizing the laser scattering and absorption at the windows. Reduced scattering translates to fewer wall interactions with the incident radiation. Minimizing the absorption by the cell windows minimizes the PAS interference caused by the periodic window heating. The magnitude of the window noise is also small because the laser power is small and the central chamber is long enough that the window heating effects dissipate before reaching the microphone.

The PAS cell was isolated from room noise by construction of one acoustical isolation box inside another. When running PAS tests, there was no noticeable difference between operation with the doors to the acoustical boxes open or closed. Therefore, at the modulation frequency of the PAS tests, room noise does not significantly contribute to the signal-to-noise ratio.

Flow noise can be eliminated by having stagnant conditions in the PAS cell [20]. For tests with particulates, this is impractical because the particulates would settle out of the gas. Therefore, flow rates are kept as low as practical, and the flow passage for the flue gas entering the cell is angled upward to reduce eddy currents, which generate acoustical noise in the cell.

External acoustical noise entering the PAS cell come from the fluidized bed combustor and the vacuum pump, with the fluidized bed combustor representing the more serious problem. Faxvog and Roessler [3] isolated their PAS apparatus from the pressure fluctuation generated from the exhaust of a diesel engine by using a constant flow dilution tube with dilution ratios of 3:1 to 10:1. The high dilution ratio damps out any pressure fluctuations that were generated by the operation of the diesel engine. Although this method worked well for their situation, the PAS signal generated by a diluted sample of flue gas would not be large enough to measure in the present apparatus.

The combustion of coal in the fluidized bed causes pressure fluctuations that propagate through the sample line; if these pressure fluctuations are not dampened, they will cause overloading of the microphone and lock-in amplifier. To reduce the effect of these pressure fluctuations, the flue gas sample passes through a muffler [35], consisting of a 3-inch pipe lined with 1-inch of fiberglass held in place by 40-mesh

stainless steel. The muffler isolates the PAS cell from high frequency ($\geq$ 1 kHz) noise generated during coal combustion and substantially dampens the low frequency noise.

The first approach to damping out the pump noise was to use a venturi instead of a vacuum pump to draw the sample through the PAS cell. Although the use of the venturi substantially reduced the magnitude of the noise, the noise was shifted to frequencies ($\geq$ 1 kHz) that overlapped the modulation frequency of the excitation source. Therefore, a vacuum pump was used to draw the sample through the PAS cell. The vacuum pump noise was damped out by adding more piping between the pump and the PAS cell and installing a valve at the suction side of the pump. This method has been proven effective for other low frequency noise applications [35] and provided significant reduction for our system (Figure 6.1).

After the noise was reduced to a workable level, a band pass filter in conjunction with a well chosen modulation frequency for the excitation source further increased the PAS sensitivity. Roessler [21] has observed that noise interferences from the exhaust of a diesel engine are greatest at low frequencies, but the PAS signal is inversely proportional to the modulation frequency. Roessler [21] found that the noise interference decreased faster than the PAS signal as the modulation frequency was increased. He concluded that 2–3 kHz was a reasonable range for operation. The same functional relationship was observed in the present application. A modulation frequency of 2 kHz was found to be a reasonable compromise between the PAS signal and noise considerations.

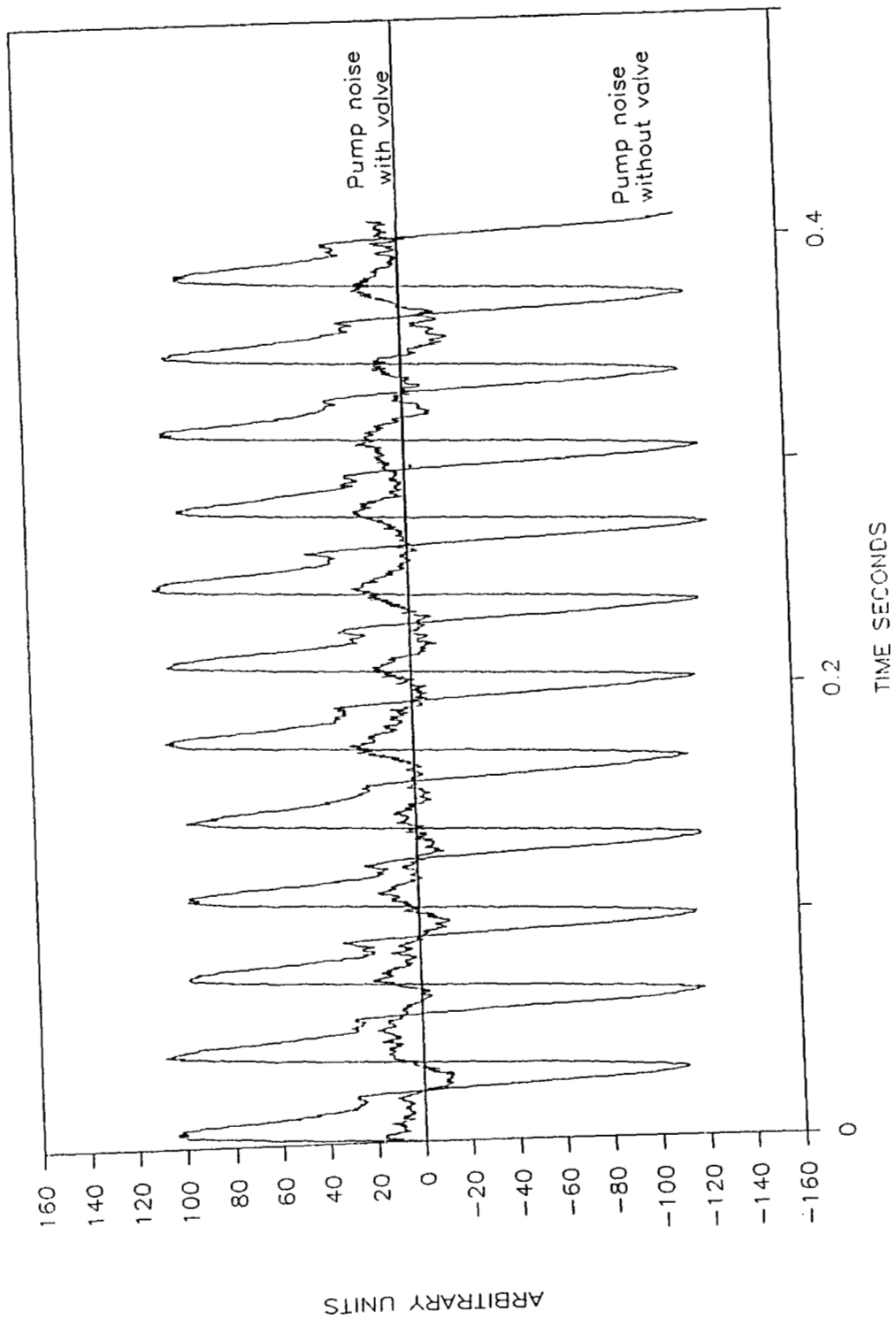

Figure 6.1: Reduction in pump noise at the microphone

6.2 PAS Cell Calibration

The two PAS cells were calibrated with 462 ppm NO_2 in N_2 ($b_a = 0.028$ m^{-1} [36]) at a chopping frequency of 2 kHz to determine which cell should be used for the carbon detection experiments. The calibration gas was pumped through a cell at different flow rates to ensure that the signal was independent of flow velocity. The flow rate through the PAS cell must be varied with combustor operating conditions to maintain isokinetic sampling. Flow rates in the range of 0.25 to 0.51 m/s were required for flue gas tests. The PAS signal generated from NO_2 in the brass cell as a function of the flow velocity is shown in Figure 6.2. The signal is essentially constant in the range of 0.25 to 0.51 m/s, the range to be used in our tests. However, the signal begins to deviate at about 0.64 m/s. The brass cell was used for the combustion tests that follow.

The aluminum cell had a cell responsivity of 3.28 mV-m/W and a signal-to-noise ratio less than 8. In comparison, the brass cell had a responsivity of 4.25 mV-m/W and a signal-to-noise ratio greater than 25. Although the brass cell is clearly superior to the aluminum cell, its responsivity is much lower than obtained by other researchers using PAS for soot detection [2, 3]. The reason for this is unclear but may be related to the size of the exit passages compared with the size of the central chamber of the cell. Other researchers using PAS typically employ smaller diameter exit passages compared to the diameter of the central chamber of the cell [2, 3]. Also, Rosengren [37] states that the pressure sensor area should not be larger than the wall area of the main chamber. The pressure area (diameter = 9.5 mm) of the microphone is approximately 6 times greater than the wall area of the main chamber (diameter = 4 mm). Accordingly, this is hypothesized to be the reason for the low

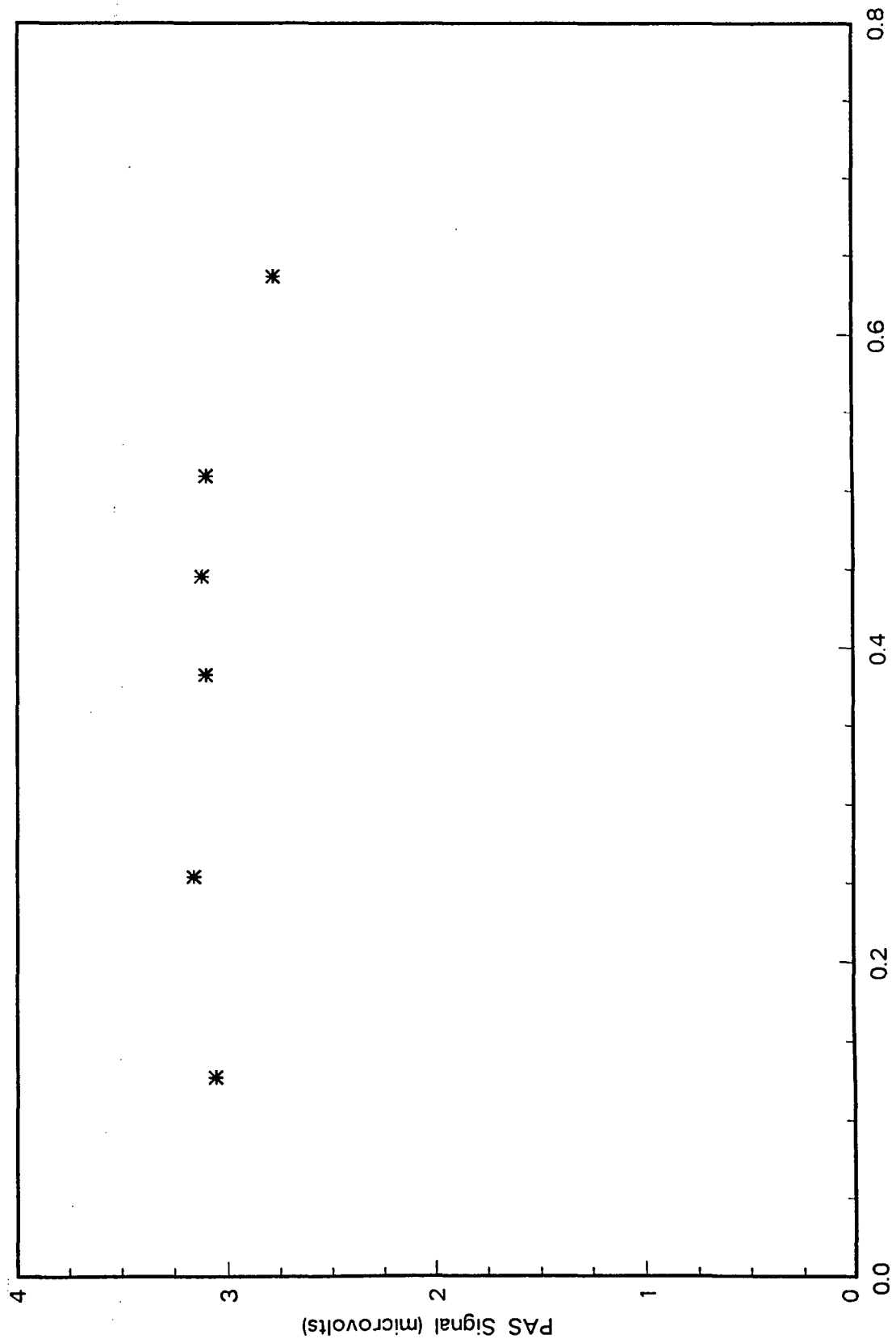

Figure 6.2: PAS signal generated from NO_2 in the brass cell as a function of the flow velocity

value of the responsivity.

6.3 Determination of Carbon Concentrations

The results of the first set of combustion tests, performed in a sand bed to which 5% limestone had been added, are shown in Figure 6.3, with test conditions listed in Table 6.1. Six distinct operating conditions, designated as Test 1 through 6, were performed. Three different mass loadings through the PAS cell were obtained for each operating condition by diluting the flue gas sample. The results indicate that the PAS signal is linear with carbon loading for a given combustor operating condition (i.e., for a given particle size distribution and morphology). However, a different line was obtained for each operating condition; a useful instrument should give a single line dependent only on the concentration of carbon in the flue gas.

It is instructive to compare these results with the PAS signal expected for unburned carbon emitted from our combustor. If the carbon particles are large spheres ($D \gg \lambda$), then the mass specific absorption cross section is given by Eq. (2.2). The integrated mass specific absorption coefficient, A_a, can be obtained by substituting Eq. (2.2) using ρ for char as approximately 1800 kg/m^3 and the mass distribution, m(D) for unburned carbon into Eq. (2.6). In the absence of the mass distribution for char, the mass distribution for fly ash (a mixture of unburned carbon and mineral matter particles), which was obtained from Microtrac analysis (see Figure 6.4), was used. This mass distribution, with an average particle diameter of 34 μm, yields an expected A_a of 0.078 m^2/g. The PAS signal predicted by Eq. (2.12) is plotted in Figure 6.3. The predicted PAS signal is in close agreement with Test 1, which was the first test performed. The agreement between prediction and experiment becomes

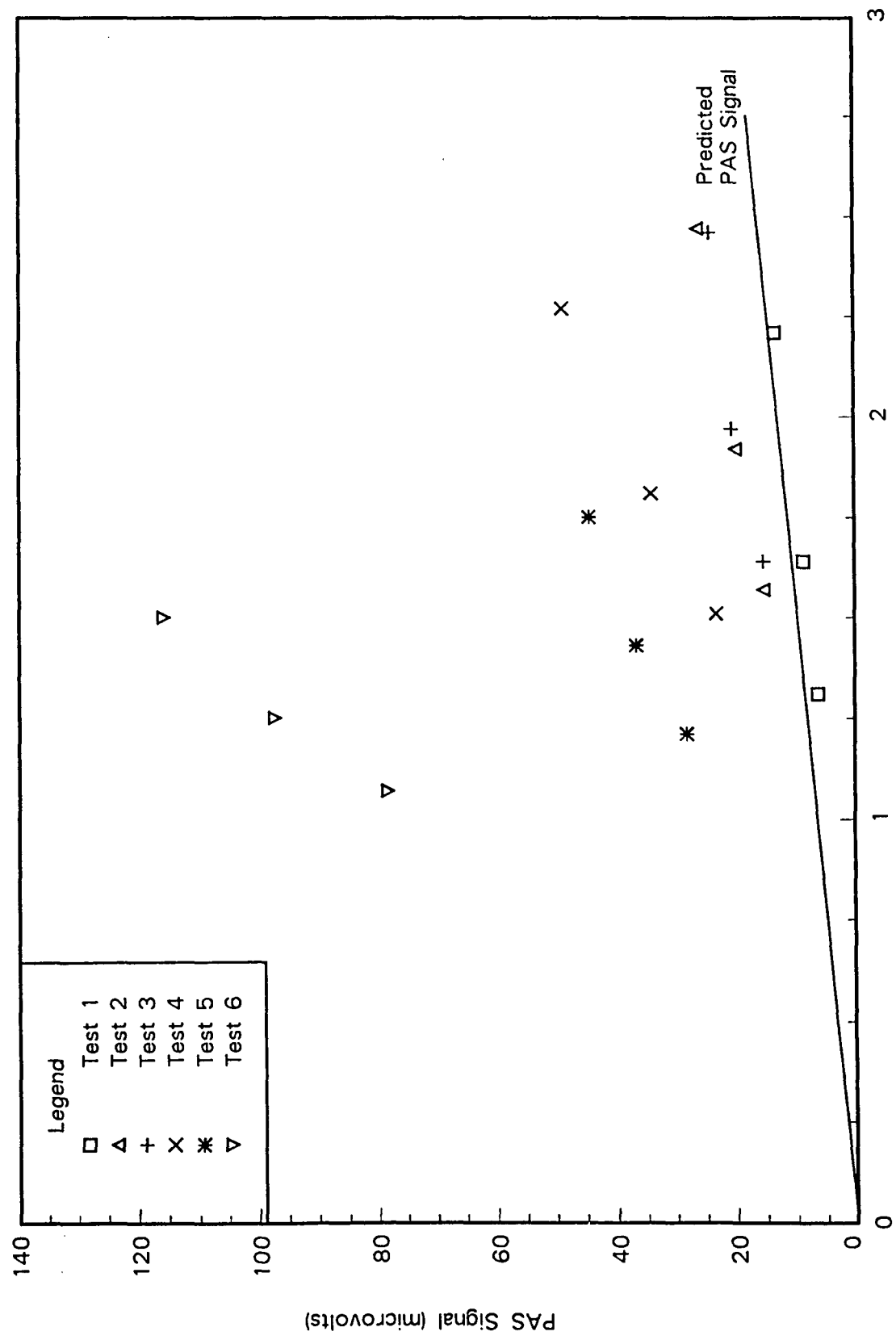

Figure 6.3: The influence of condensed tar on the PAS signal

Table 6.1: Combustion conditions—sand bed

	Bed Temp (°F)	Gas Velocity (m/s)	Flue Gas Oxygen (%)	Total Loading (g/m^3)	Carbon Percent (%)	Carbon Loading (g/m^3)	PAS Signal (μV)
Test 1	1550	0.72	4.2	2.00	63.4	1.31	6.36
				2.59		1.64	8.75
				3.49		2.21	13.40
Test 2	1630	0.93	4.6	2.63	59.7	1.57	15.40
				3.22		1.92	19.98
				4.14		2.47	26.30
Test 3	1690	1.14	3.4	3.13	52.4	1.64	15.37
				3.76		1.97	20.62
				4.69		2.46	24.28
Test 4	1750	1.15	4.0	2.79	54.1	1.51	23.20
				3.35		1.81	34.14
				4.20		2.27	48.92
Test 5	1800	1.37	4.4	2.99	40.5	1.21	28.30
				3.53		1.43	36.67
				4.32		1.75	44.43
Test 6	1880	1.59	3.7	3.57	30.0	1.07	78.45
				4.17		1.25	97.30
				5.00		1.50	115.68

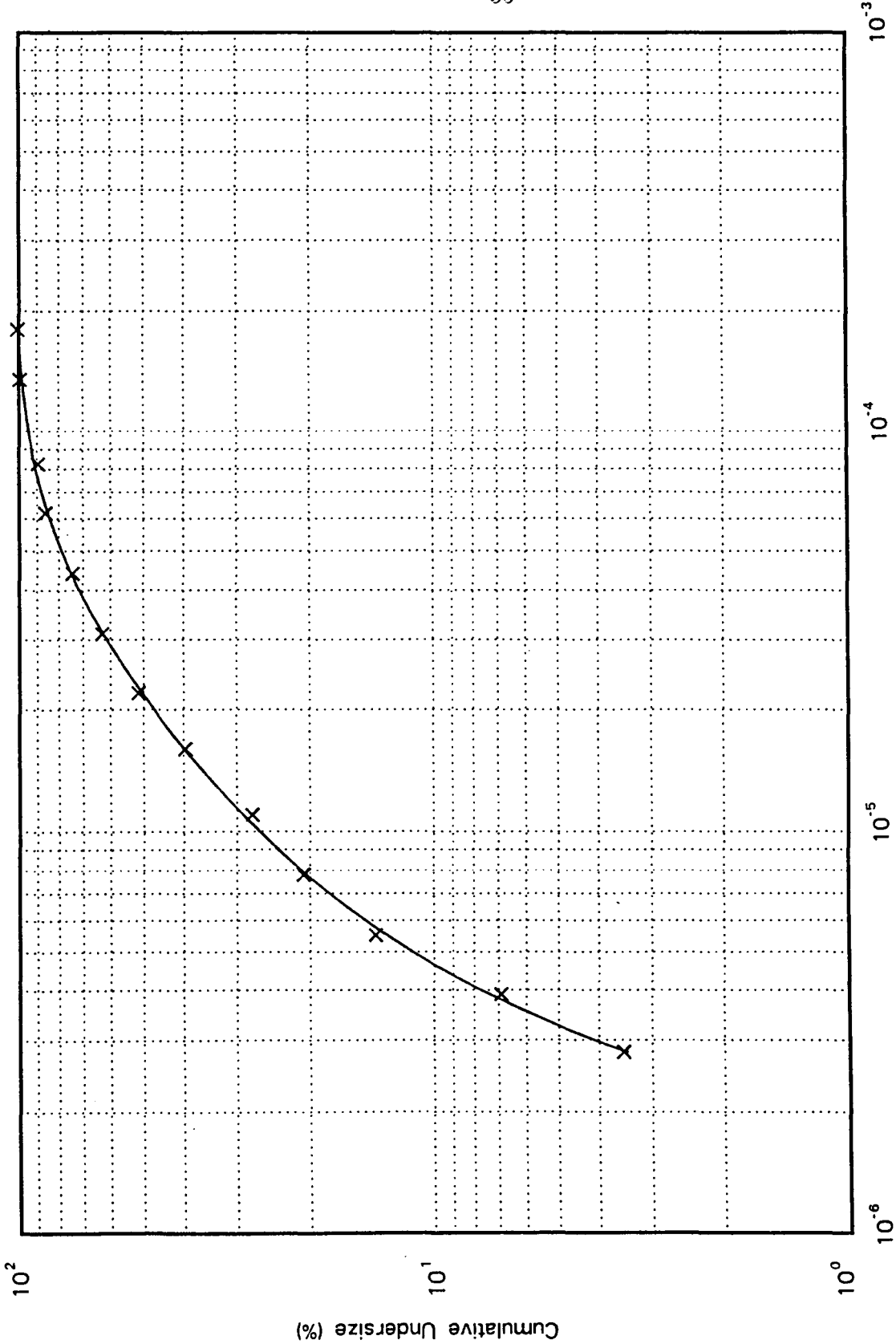

Figure 6.4: Mass distribution of the fly ash

progressively worse for subsequent tests, especially for Tests 4 to 6. Additional tests were performed to investigate this discrepancy.

The first test was to determine whether gas or particles produced the excessively large PAS signals. When a particulate filter was placed in the gas line before the PAS cell, the signal dropped below the detection limit of the system (1 μV). Accordingly, the signal was not due to gaseous combustion products but was arising from particulate matter or liquid droplets in the flue gas.

The PAS signal increased monotonically from Test 1 to 6. This behavior may be correlated to either temperature of superficial velocity through the combustor; however, the PAS signal may instead correlate with the time elapsed between the performance of a test and the initial charging of the bed with 5% limestone. The hypothesis was that a significant fraction of this small quantity of limestone was attrited and elutriated from the bed before completion of the test series which had two consequences. First, uncalcined limestone collected in the cyclone can increase LOI. The result is overestimation of carbon concentrations in the flue gas. This error manifests itself as PAS plots with a negative y-intercepts, a phenomenon evident in some of the experimental data of Figure 6.3. Second, the tar content of the flue gas will increase with time as the quantity of limestone in the bed decreases. Condensed tar, which increases from Test 1 to 6, due to reduction in the limestone and the increase in bed temperature [34], might produce significant PAS signals. This hypothesis was tested by bringing the combustor to steady-state after Test 6 and recording the PAS signal. At this point, 1.5 kg of limestone was injected into the combustor to catalyze the destruction of tars. As limestone was added, the PAS signal dropped by 90%, to a level comparable with those of Tests 1 through 3. Therefore,

Table 6.2: Combustion conditions—limestone bed

	Bed Temp (°F)	Gas Velocity (m/s)	Flue Gas Oxygen (%)	Total Loading (g/m^3)	Carbon Percent (%)	Carbon Loading (g/m^3)	PAS Signal (μV)
Test 9	1720	1.44	4.9	7.30	32.8	2.40	9.86
Test 10	1680	1.23	5.3	7.44	38.3	2.85	12.33
Test 11	1630	1.03	5.0	6.93	44.9	3.11	13.65
Test 12	1550	0.83	5.1	6.87	55.9	3.84	8.57
Test 13	1750	1.52	5.0	6.73	31.2	2.09	9.18
Test 14	1760	1.37	4.4	7.42	32.8	2.44	10.32

the conclusion was that the condensed tars significantly influenced PAS signals.

Tar is not a normal constituent of flue gas from industrial- and utility-scale boilers [27, 38, 39]. It appears in our experiments as an artifact of the uninsulated freeboard of the laboratory-scale combustor. Accordingly, additional tests were performed to exclude both tar and uncalcined limestone from the flue gas. The second set of tests (Tests 9–12) employed a bed of 69% calcined and/or sulfated limestone and 31% sand. Test conditions are presented in Table 6.2.

Figure 6.5 shows that Tests 9–11 are well correlated to a straight line intersecting the origin. The slope of this line yields an integrated mass specific absorption coefficient of 0.0389 m^2/g, which is within 50% of the value predicted from the mass distribution of the fly ash. Test 12, which was performed at the lowest temperature and superficial velocity, produced a PAS signal much lower than expected when

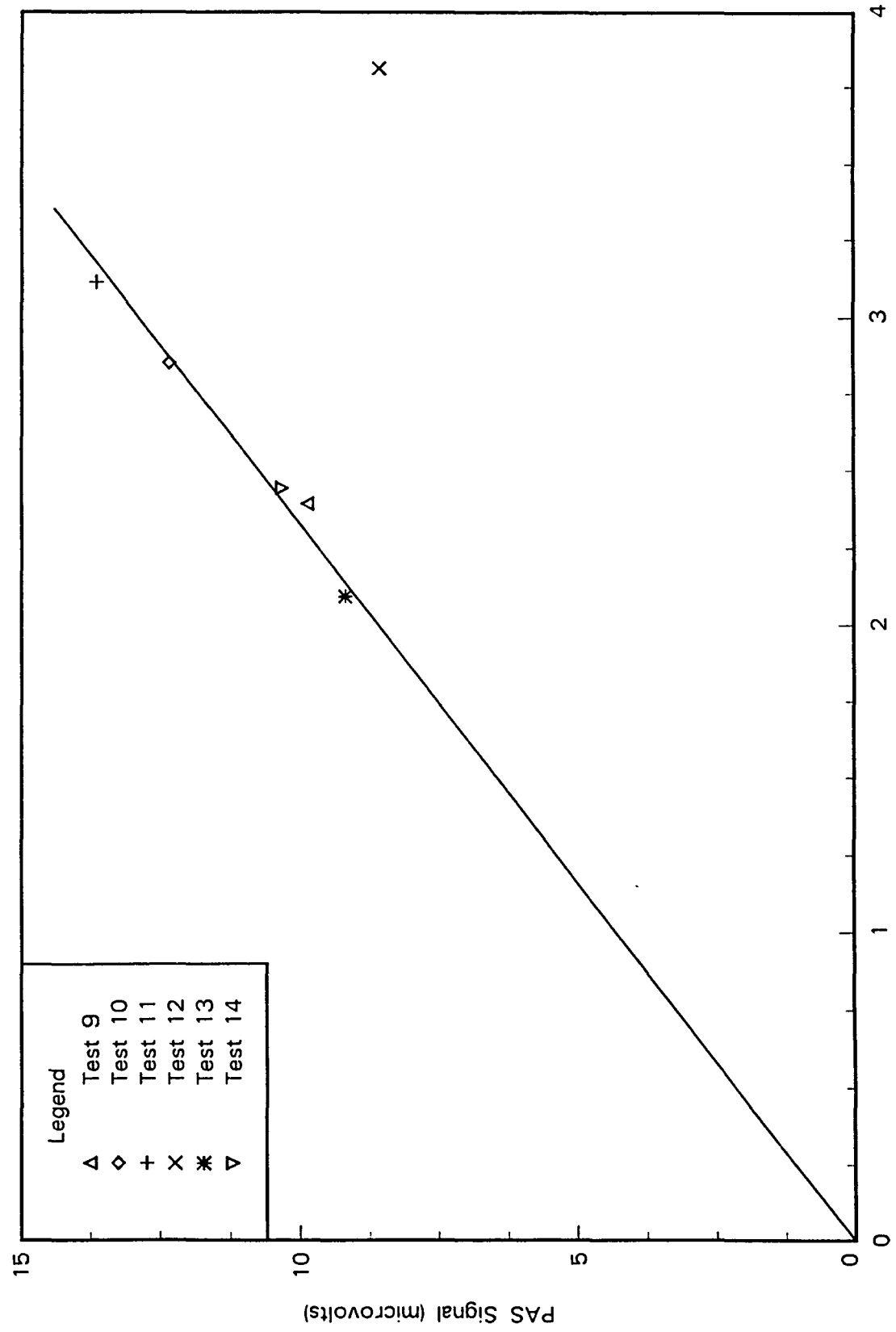

Figure 6.5: The PAS signal

compared with the other tests. Scanning electron microscopy (SEM) was performed on fly ash samples obtained in Tests 9 and 12 (Figures 6.6 and 6.7, respectively) to understand this abnormality. Light colored particles in the photographs are mineral matter, gray particles are unburned carbon, and the black material is mounting epoxy. Examination of these photographs suggest that low temperatures (Test 12) result in carbon particles roughly rectangular in shape, many with length-to-width ratios of 3 to 1, whereas higher temperatures (Test 9) produce carbon particles that are more spherical, although still irregularly shaped. From examination of the photographs, the average size of particles in Test 12 appears to be larger than for Test 9. The larger sizes of particles in Test 12 will yield a lower mass specific absorption coefficient than smaller, spherical particles and may explain the smaller PAS signalof Test 12. From the photographs, the unburned carbon generally appears as discrete particles, although some composite particles of carbon and mineral matter appear in the photographs.

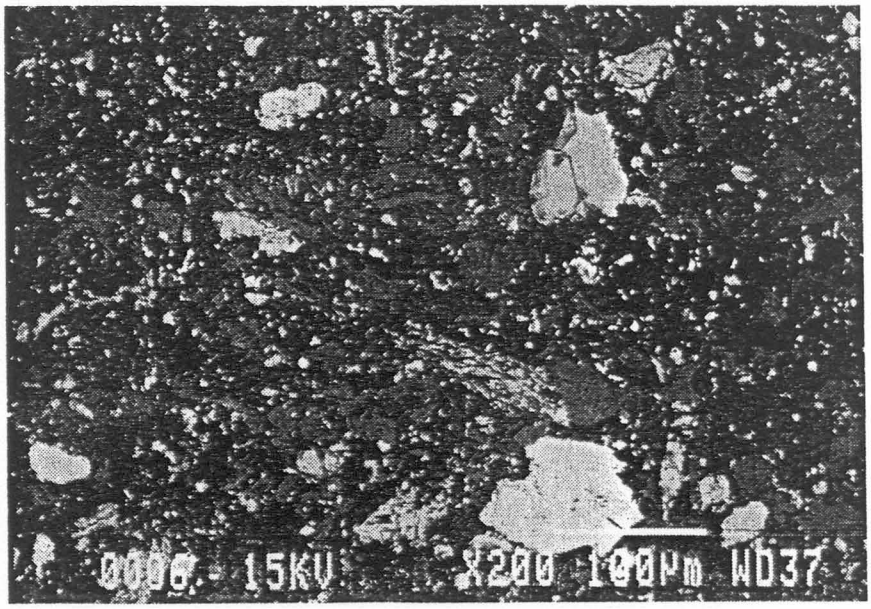

Figure 6.6: Fly ash from Test 9

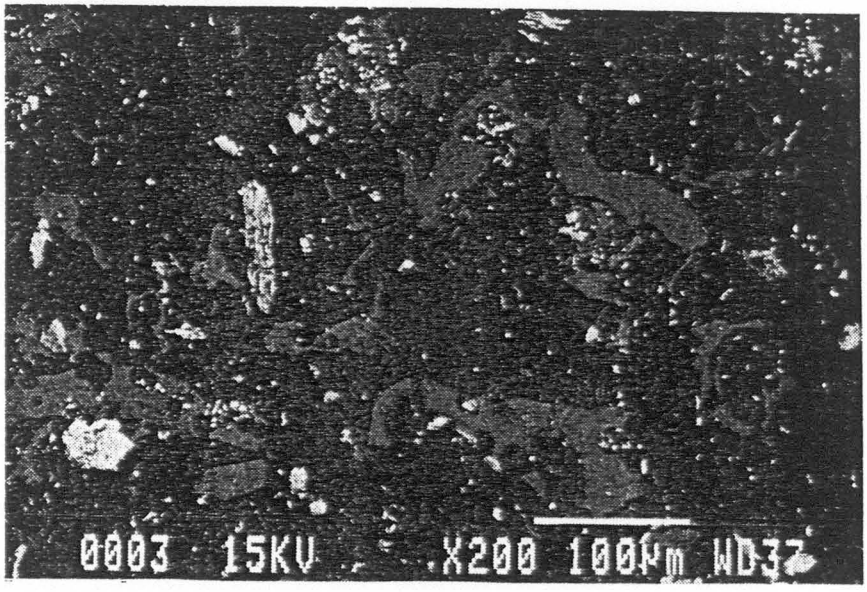

Figure 6.7: Fly ash from Test 12

7. CONCLUSIONS

The first set of tests shows that PAS signals are strongly influenced by condensed tars in the flue gas sample. However, tar is not usually found in industrial-scale boilers and should not diminish the utility of PAS for detection of unburned carbon in such applications. In tests where tar was absent from the flue gas, a linear PAS response with carbon concentration was obtained that agreed with theoretical expectations. The only exception occurred for a test that produced carbon particles non-spherical in shape.

Further research is required to determine the shape and morphology of fly ash expected from industrial-scale boilers. If irregular shapes are commonly encountered, then a longer wavelength excitation source, such as microwaves, will be required for the carbon monitor to achieve a linear PAS signal with changes in carbon concentrations. Also, the effect of shading of the carbon by mineral matter due to the heterogeneous composition of some of the particles needs to be resolved.

Improvements in the signal-to-noise ratio can be achieved by increasing the power of the excitation source. The increase in power provides a direct gain in the PAS signal without increasing the noise substantially because the major source of noise comes from the combustor and not window or cell wall noise.

The signal-to-noise ratio of the aluminum PAS cell was increased from 2 (Dona

and Brown [4, 5]) to 8. This was further increased to over 25 with the brass PAS cell. Additional improvements in the signal-to-noise can be achieved by reducing the combustion noise that propagates through the sample line into the PAS cell. The combustion noise can be eliminated by operating the PAS apparatus off-line; if this is to be done, a practical way of entraining fly ash in air needs to be developed.

8. BIBLIOGRAPHY

[1] "Standard Test Method for Ash in the Analysis of Coal and Coke." *ASTM Standard No. d3174-82,* Annual Book of ASTM Standards Part 26. ASTM, Philadelphia, 1982.

[2] Japar, S. M. and Szkarlat, A. C. "Measurement of Diesel Vehicle Exhaust Particulate Using Photoacoustic Spectroscopy." *Combust. Sci. Tech.,* 24, 215, 1981.

[3] Faxvog, F. R. and Roessler, D. M. "Optoacoustic Measurements of Diesel Particulate Emissions." *J. Appl. Phys.,* 50, 7880, 1979.

[4] Dona, A. R. "Photoacoustic Detection of Unburned Carbon in Airborne Fly Ash." M. S. thesis. Iowa State University, Ames, Iowa, 1988.

[5] Brown, R. C., and Dona, A. R. "On-Line Determination of Unburned Carbon in Airborne Fly Ash." *Fossil Fuels Combustion Symposium,* Energy Sources Technology Conference and Exhibition, Houston, TX, Jan. 22-26, 1989. ASME: New York.

[6] Roessler, D. M. "Photoacoustic Insights on Diesel Exhaust Particles." *Sci. Total Environ.,* 36, 183, 1984.

[7] Pao, Y. H. *Optoacoustic Spectroscopy and Detection.* Academic Press, New York, 1977.

[8] Rosencwaig, A. *Photoacoustics and Photoacoustic Spectroscopy.* Wiley, New York, 1980.

[9] Faxvog, F. R. and Roessler, D. M. "Carbon Aerosol Visibility vs Particle Size Distribution." *Appl. Opt.,* 17, 2612, 1978.

[10] Roessler, D. M. and Faxvog, F. R. "Opacity of Black Smoke: Calculated Variation with Particle Size and Refractive Index." *Appl. Opt.,* 18, 1399, 1979.

[11] Jones, A. R. "Scattering of Electromagnetic Radiation in Particulate Laden Fluids." *Prog. Energy Combust. Sci.,* 5, 73, 1979.

[12] Hawksley, P. G. W., Badzioch, S., and Blackett, J. H. *Measurement of Solids in Flue Gases.* The Institute of Fuel, London, 1977.

[13] Roessler, D. M. and Faxvog, F. R. "Optoacoustic Measurement of Optical Absorption in Acetylene Smoke." *J. Opt. Soc. Am.,* 69, 1699, 1979.

[14] Adams, K. M. "Real-Time in situ Measurements of Atmospheric Optical Absorption in the Visible via Photoacoustic Spectroscopy. 1: Evaluation of Photoacoustic cells." *Appl. Opt.,* 27, 4052, 1988.

[15] Terhune, R. W. and Anderson, J. E. "Spectrophone Measurements of the Absorption of Visible Light by Aerosols in the Atmosphere." *Optics Letters,* 1, 70, 1977.

[16] Japar, S. M. and Szkarlat, A. C. "Real-Time Measurements of Diesel Vehicle Exhaust Particulate Using Photoacoustic Spectroscopy and Total Light Extinction." *Trans. SAE,* 90, 3624, 1982.

[17] Roessler, D. M. "Diesel Particle Mass Concentration by Optical Techniques." *Appl. Opt.,* 21, 4077, 1982.

[18] Roessler, D. M. and Faxvog, F. R. "Changes in Diesel Particulates with Engine Air/Fuel Ratio." *Combust. Sci. Tech.,* 26, 225, 1981.

[19] Japar, S. M., Szkarlat, A. C., and Pierson, W. R. "The Determination of the Optical Properties of Airborne Particle Emissions from Diesel Vehicles." *Sci. Total Environ.,* 36, 121, 1984.

[20] Osada, H, Okayama, J., Ishida, K., and Saitoh, O. "Real-Time Measurement of Diesel Particulate Emissions by the PAS method Using a CO_2 Laser." *SAE Paper 820461,* 1983.

[21] Roessler, D. M. "Photoacoustic Insights on Diesel Exhaust Particles." *Appl. Opt.,* 23, 1148, 1984.

[22] Adams, K. M., Davis, L. I., Japar, S. M., and Pierson, W. R. "Real-Time, in situ Measurements of Atmospheric Optical Adsorption in the Visible Via Photoacoustic Spectroscopy—II. Validation for Atmospheric Elemental C arbon Aerosol." *Atmospherical Environment,* 23, 693, 1989.

[23] Vorres, K. S. *Mineral Matter and Ash in Coal.* American Chemical Society, Washington, DC, 1986.

[24] Bryers, R. W. *Ash Deposits and Corrosion Due to Impurities in Combustion Gases.* Hemisphere Publishing, Washington, DC, 1978.

[25] Donsi, G., Massimilla, L., and Miccio, M. "Carbon Fines Production and Elutriation from the Bed of a Fluidized Coal Combustor." *Combustion and Flame,* 41, 57, 1981.

[26] Vann Bush, P., Snyder, T. R., and Smith, W. B. "Filtration Properties of Fly Ash from Fluidized Bed Combustion." *JAPAC,* 37, 1292, 1987.

[27] Gay, A. J. and Frigge, J. "Characterisation of Fly Ash from Fluidised Coal Combustors with Regard to its Utilisation and Safe Disposal." *Flue Gas and Fly Ash.* Elsevier Science Publishers LTD, England, 1989.

[28] Poersch, W. W. "Short Communication." *Powder Technology,* 40, 331, 1984.

[29] Merrick, D. and Highley, J. "Particle Size Reduction and Elutriation in a Fluidized Bed Process." *AICHE Symposium Series,* No. 137, Vol. 70, 1974.

[30] Chirone, R., Cammarota, A., Ď Amore, M., and Massimilla, L. "Elutriation of Attrited Carbon Fines in the Fluidized Combustion of a Coal." *Nineteenth Symposium on Combustion.* The Combustion Institute, Pittsburgh, Pennsylvania, 1982.

[31] Aulisio, C. Divilio, R., and Reed R. "Results of Recent Test Program Related to AFB Combustion Efficiency." *The Proceedings of the Fifth International Conference of Fluidized Bed Combustion,* Washington, DC, Vol . III, 1978.

[32] Klemm, K. and Liphard, K. G. "Adsorption and Desorption Phenomena of Polycyclic aromatic Hydrocarbons on Fly Ash." *Flue Gas and Fly Ash* Elsevier Science Publishers LTD., England, 1989.

[33] Gregory, J. and Brown, R. C. "Combustion Behavior of Coal-Water-Mixtures in Fluidized Beds." *Proc.* 10^th *Int. Conf. on Fluidized Bed Combustion,* San Francisco, Calif., 1989.

[34] Huseyin, V., Walsh, P. M., Sarofim, A. F., and Beer, J. M. "Destruction of Tar During Oxidative and Nonoxidative Pyrolysis of Bituminous Coal in a Fluidized Bed." *Combust. Sci. Tech.,* 63, 229, 1989.

[35] Pish, R. H., Sparks, C. R., Ajax, M. F., Brown, M. E., and Saathoff, D. R. *Handbook for Noise Control at Gas Pipeline Facilities.* San Antonio, Texas, 1977.

[36] Hsu, D. K., Monts, D. L., and Zare, R. N. *Spectral Atlas of Nitrogen Dioxide 5530 to 6480 Å.* Academic Press, New York, 1978.

[37] Rosengren, L. "Optimal Optoacoustic Detector Design." *Appl. Opt.,* 23, 1148, 1984.

[38] Fisher, G. L., Prentice, B. A., Silberman, D., Ondov, J. M. Biermann A. H., Ragaini, R. C., and Mc Farland A. R. "Physical and Morphological Studies of Size-Classified Coal Fly Ash." *Environ. Sci. Technol.,* 12, 447, 1978.

[39] Odler, I. and Zysk, K. H. "Investigations on the Composition of Individual Fly Ash and CFB-Ash Particles." **In** *Fly Ash and Coal Conversion By-Products: Characterization Utilization and Disposal V.* Materials Research Society, Pittsburgh, Pennsylvania, 1989.